Comparison of Rheometric Devices for Measuring the Rheological Parameters of Debris Flow Slurry

YANG Hong-juan[1] http://orcid.org/0000-0003-0635-6764; e-mail: yanghj@imde.ac.cn

WEI Fang-qiang[2] http://orcid.org/0000-0001-8734-0881; ✉ e-mail: fqwei@imde.ac.cn

HU Kai-heng[2] http://orcid.org/0000-0001-8114-5743; e-mail: khhu@imde.ac.cn

ZHOU Gong-dan[2] http://orcid.org/0000-0001-9014-2931; e-mail: gordon@imde.ac.cn

LYU Juan[2] http://orcid.org/0000-0003-2894-4647; e-mail: ljuan@imde.ac.cn

1 Key Laboratory of Mountain Hazards and Earth Surface Process, Chinese Academy of Sciences, Chengdu 610041, China

2 Institute of Mountain Hazards and Environment, Chinese Academy of Sciences, Chengdu 610041, China

Abstract: Soil samples with clay content ranging from 15% to 31%, were taken from three debris flow gullies in Southwest China. Three debris flow slurry samples were prepared and tested with four measuring systems of an Anton Paar Physica MCR301 rheometer, including the concentric cylinder system, the parallel-plate system, the vane geometry, and the ball measuring system. All systems were smooth-walled. Flow curves were plotted and yield stress was determined using the Herschel-Bulkley model, showing differences among the different systems. Flow curves from the concentric cylinder and parallel-plate systems involved two distinct regions, the low shear and the high shear regions. Yield stresses determined by data fitting in the low shear region were significantly lower than the values from the inclined channel test which is a practical method for determining yield stress. Flow curves in the high shear region are close to those from the vane geometry and the ball measuring system. The fitted values of yield stress are comparable to the values from the inclined channel test. The differences are caused by wall-slip effects in the low shear region.

Vane geometry can capture the stress overshoot phenomenon caused by the destruction of slurry structure, whereas end effects should be considered in the determination of yield stress. The ball measuring system can give reasonable results, and it is applicable for rheological testing of debris flow slurries.

Introduction

Rheological parameters are crucial in debris flow dynamics, especially in the simulation of debris flow as continuum media. At present, however, the rheology is limited to the fine part of the flow, i.e. the slurry composed of clay grains, although the coarse particles also contribute to rheological features.

Rheometers are instruments used to make rheological measurements. They generally consist of rotors and static walls with the sample being sheared when the rotor rotates. The rotor is absent

in some rheometers such as the pipe viscometer. Normally shear rate is proportional to the rotational speed, and the drag force exerted on the rotor is obtained by measuring the torque. Concentric cylinder systems (CCS) are commonly used for rheological measurement of mud slurry (e.g., O'Brien and Julien 1988; Major and Pierson 1992; Huang and Adobe 2009). Shear rate can vary over a wide range and sample temperature is easy to control with this system. However, wall slip is common when measuring particle suspensions. Moreover, it is difficult to derive accurate shear rates because the distribution of shear stress is heterogeneous in the gap (Nguyen and Boger 1987; Yeow et al. 2000; Ancey 2005). Parallel-plate systems (PPS) are also frequently used for particle suspensions (Chan and Powell 1984; Coussot 1995; Wang et al. 2004). They are easy to operate and the shear rate is easy to determine. As with CCS, wall slip can occur. It can be overcome, to some extent, by wall roughening or profiling (Barnes 1995; Ancey and Jorrot 2001). The cone-and-plate system (CPS), with its homogeneous shear rate in the gap, can provide highly accurate rheological data but it is not applicable for debris flow slurry because of the narrow gap in commercial CPS rheometers. Some researchers have developed large-scale CPS to test particle suspensions (e.g., Shen 1998; Contreras and Davies 2000; Boyer et al. 2011).

In vane geometry, a thin-bladed vane is used as the rotor instead of the solid cylinder in CCS, and slip effects can be eliminated (Duan and Sun 2001). In addition, the structure of the sample can be preserved when the vane is introduced into the sample. Originally, this geometry was used to measure yield stress, but more recently it also has been used to measure other rheological parameters (Barnes and Nguyen 2001). Huang et al. (2005) studied the transition from frictional to lubricated flows of a dense particle suspension with vane geometry. Sosio and Crosta (2009) used the vane geometry to measure rheological parameters of mud slurries with different particle size distributions and different concentrations. Müller et al. (1999) developed a ball measuring system (BMS) to overcome the particle size limit of conventional systems. Schatzmann et al. (2009) studied relationships between the measured data, rotational speed and torque, and the rheological

data, shear rate and shear stress, using Newtonian, Power law, and yield stress fluids, respectively, and applied the BMS to sediment-water mixtures. However, the question of whether the vane geometry and the BMS are more appropriate than conventional systems for testing debris flow slurry remains unresolved. Therefore, we prepared simulated debris flow slurries and tested them with the CCS, PPS, vane geometry, and the BMS, respectively. Then we compared the resulting rheological data and evaluated the applicability of each system for debris flow slurry analysis.

1 Experimental setup

An Anton Paar Physica MCR301 rheometer was used in this study. It can operate in both stress-controlled and rate-controlled modes. The rheometer has a range of torque $10^{-7}\sim0.2$ Nm and a range of rotational speed $10^{-6}\sim3000$ min^{-1}. Four smooth-walled measuring systems including the CCS, the PPS, the vane geometry, and the BMS were compared. Wall roughening can restrain wall slip effects during the rheological test. However, the roughened surface can also disturb the laminar flow conditions of fluids, and turbulent flow conditions are produced causing vortices in the boundary layer between the liquid sample and the wall surface (Mezger 2006). Therefore none of the systems were roughened for the present study.

1.1 Concentric cylinder system (CCS)

The CCS is composed of two cylinders with the inner one as rotor and the outer one as cup. The inner radius is r_i=15.215 mm, the length is L=45.6 mm, and the outer radius is r_o=21.001 mm. Shear stress decreases in the gap from the inner cylinder to the outer cylinder as:

$$\tau=\frac{T}{2\pi r^2 L} \qquad (1)$$

in which T is the torque and r is the position along the radius of r_o. The following relationship exists between the angular velocity ω, shear stress τ, and shear rate $\dot{\gamma}$ (Nguyen and Boger 1987):

$$\omega=\frac{1}{2}\int_{\max(\tau_o,\tau_y)}^{\tau_i}\frac{\dot{\gamma}}{\tau}d\tau \qquad (2)$$

where τ_y is the yield stress; τ_i and τ_o are shear stresses at the inner and outer walls of the gap separately.

The analytical expression of $\dot{\gamma}$ can be derived from Eq. 2 for some specific fluids such as Newtonian fluid and Bingham fluid. Many researchers (e.g., Yang and Krieger 1978; Ren 1995) have studied the determination of $\dot{\gamma}$ for complex fluids and Yeow et al. (2000) developed a method based on Tikhonov regularization, which does not require any predefined τ-$\dot{\gamma}$ relationship and applies equally well to fluids with and without yield stress. This method was used in the present study.

The CCS was calibrated with standard silicon oil to eliminate end effects before use. We used the following procedure: (1) measure the $T\sim\omega$ curve of the silicon oil; (2) obtain the τ-$\dot{\gamma}$ curve from the $T\sim\omega$ data with the method developed by Yeow et al. (2000); (3) determine the viscosity of the silicon oil by fitting the τ and $\dot{\gamma}$ data. The modified torque value T_m is then:

$$T_m = \frac{\eta_a}{\eta_f} T_o \qquad (3)$$

where η_a is the actual viscosity of the silicon oil, η_f is the fitted viscosity, and T_o is the original torque value. The ratio of η_a to η_f is defined as the correction factor for torque. Experimental results demonstrated that it has a value of 0.909.

1.2 Parallel-plate system (PPS)

The PPS is composed of two parallel plates with the upper one as rotor (R=24.986 mm) and the lower one fixed. Shear rate increases from the center to the edge as:

$$\dot{\gamma} = \frac{r\omega}{h} \qquad (4)$$

where h is the gap width. The torque T exerted on the rotor is:

$$T = \frac{2}{3}\pi R^3 \tau_y + \frac{2}{n+3} \cdot \frac{\pi K R^{n+3} \omega^n}{h^n} \qquad (5)$$

under the assumption of the Herschel-Bulkley model for the rheology:

$$\tau = \tau_y + K\dot{\gamma}^n \qquad (6)$$

in which K is the consistency index and n is the flow behavior index.

Parameters τ_y, K, and n can be determined by the measured data T and ω following Eq. 5. Then shear stress at the edge of the plates can be computed with Eq. 6. It should be modified according to the relative magnitude of the measured and regressed values of T:

$$\tau_m = \frac{T_o}{T_r} \tau_c \qquad (7)$$

where T_o is the original torque value, T_r is the regressed torque value with Eq. 5, τ_c is the computed stress value with Eq. 6, and τ_m is the modified stress value.

1.3 Vane geometry

The vane geometry consists of a four-bladed vane and a measuring cup. The cylinder defined by the tips of the blades has a radius of r_i=11.01 mm and a length of L=16 mm. Radius of the measuring cup is r_o=21.001 mm.

The vane geometry can be treated as a CCS composed of an inner cylinder formed by the rotating vane and a measuring cup as the outer cylinder (Barnes and Nguyen 2001). Then Eq. 1 and 2 also apply to the vane geometry. However, the torque exerted on the vane is smaller than the equivalent CCS. The difference becomes smaller with the number of blades in the vane (Ovarlez et al. 2011). Therefore, the vane geometry was calibrated with standard silicon oil before use with the same procedure as the CCS, and experimental results show that the correction factor for torque equals to 1.097.

1.4 Ball measuring system (BMS)

The BMS consists of a ball fixed onto a thin holder as rotor and a cylinder as the container. Radius of the ball is D=12 mm, while the container has a radius of r_c=57.5 mm and a depth of H_c=48 mm. Distance between the ball and the container wall is 17 mm, and distance between the ball and the container bottom is 22 mm. When the ball is rotated in the fluid, shear stress is proportional to torque and shear rate is proportional to angular velocity (Schatzmann et al. 2009):

$$\dot{\gamma} = K_\omega \omega \qquad (8)$$

$$\tau = K_{\mathrm{T}}T \qquad (9)$$

in which $K_\omega=4.074$ is the conversion factor between ω and $\dot\gamma$, and K_{T} is the conversion factor between T and τ, which is related with sphere Reynolds number Re:

$$Re \le 1 \quad K_{\mathrm{T}} = 15000$$
$$Re > 1 \quad K_{\mathrm{T}} = 6603 + 8790 \cdot \exp(-0.021948 Re) \qquad (10)$$

and the Reynolds number is defined as:

$$Re = \frac{r\omega D\rho}{\eta} \qquad (11)$$

where r is the radius of the center sphere path, ρ is the density of the sample, and η is the apparent viscosity of the sample defined as the ratio of shear stress to shear rate. Since a shear stress value is needed to compute the apparent viscosity and thus the Reynolds number, iterative computation should be performed in the determination of K_{T}.

2 Materials and Experimental Procedure

2.1 Materials

Soil samples were taken from three debris flow gullies in Southwest China, including Shenxi Gully, Hongchun Gully, and Aizi Gully, and were labeled S1, S2, and S3. The particle density of the three samples was 2744 kg/m3, 2666k g/m3, and 2708 kg/m3 respectively. The particle size distribution was obtained with a Malvern Mastersizer 2000 (Figure 1). Particles of S1 were the finest with the median diameter of 0.011 mm, while particles of S3 were the coarsest with the median diameter of 0.03 mm.

When a particle suspension is sheared particle segregation (particle settling and migration) may occur. The particle segregation depends on the solid concentration, grain size distribution, type/shape of particles, as well as the shear rate and the applied rheometric system. The flow is strongly influenced by the distribution of solids concentration (Martino and Papa 2008). This influence plays a less significant role as the solid concentration increases (Vanoni 1975). In very concentrated particle fluids which are rich in fine material, particle settling can be often rendered negligible within the limited duration of the shear flow (Coussot 1997). To restrain particle segregation during the test, debris flow slurries prepared with the three soil samples had relatively high volumetric solid concentrations, with values of 40% for S1, 45% for S2, and 48% for S3.

2.2 Experimental procedure

Quantitative soil and purified water were mixed to prepare simulated debris flow slurries. These slurries were left undisturbed for 24 h to guarantee that the soil particles were thoroughly wetted. Before testing the slurry was mixed for 5 min once again.

The rheological experiments include measurements of flow curve and yield stress. The flow curve measurement involved four steps: (1) put a measured volume of sample into the container (different volumes are required in different systems); (2) lower the rotor to the measuring position; (3) leave the sample at rest for 2 min to release stress induced in step (2); and (4) record the torque data at a series of defined angular velocities. The yield stress measurement contains the above-mentioned steps (1)-(3), and the last step is increasing the torque from zero to a certain value along a linear ramp and recording the corresponding value of shear strain. A circulating water bath was used to maintain the sample temperature at 20±1°C. The total duration was about 7 min for each test and no obvious particle settling was observed.

For the PPS, gap width h should be at least 5 times larger than the largest of the particles (Mezger 2006). So h=1 mm, 2 mm, and 2.5 mm was used for S1, S2, and S3 respectively.
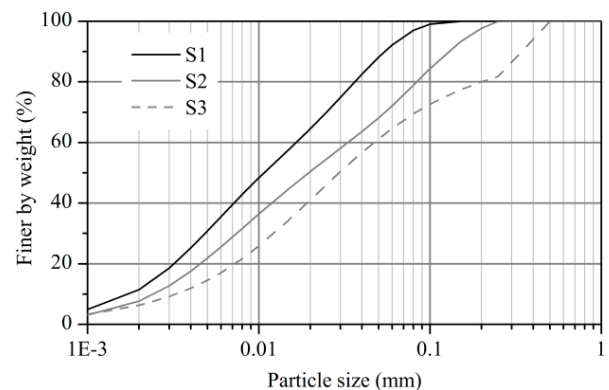
Figure 1 Particle size distribution of the experimental soil sample.

3 Results and Discussions

In order to know the repeatability of the experiment, S1 was tested twice with each system. The results have a reproducibility of less than 10%. For the other two samples, the test was only performed once.

3.1 Angular velocity and torque

The original measured data of the rheometer were angular velocity and torque, as shown in Figure 2. With the CCS, the vane, and the BMS, torque level of S3 was the lowest, while levels of S1 and S2 are close to each other. Gap width of the PPS was 1 mm when testing S1, while the value was
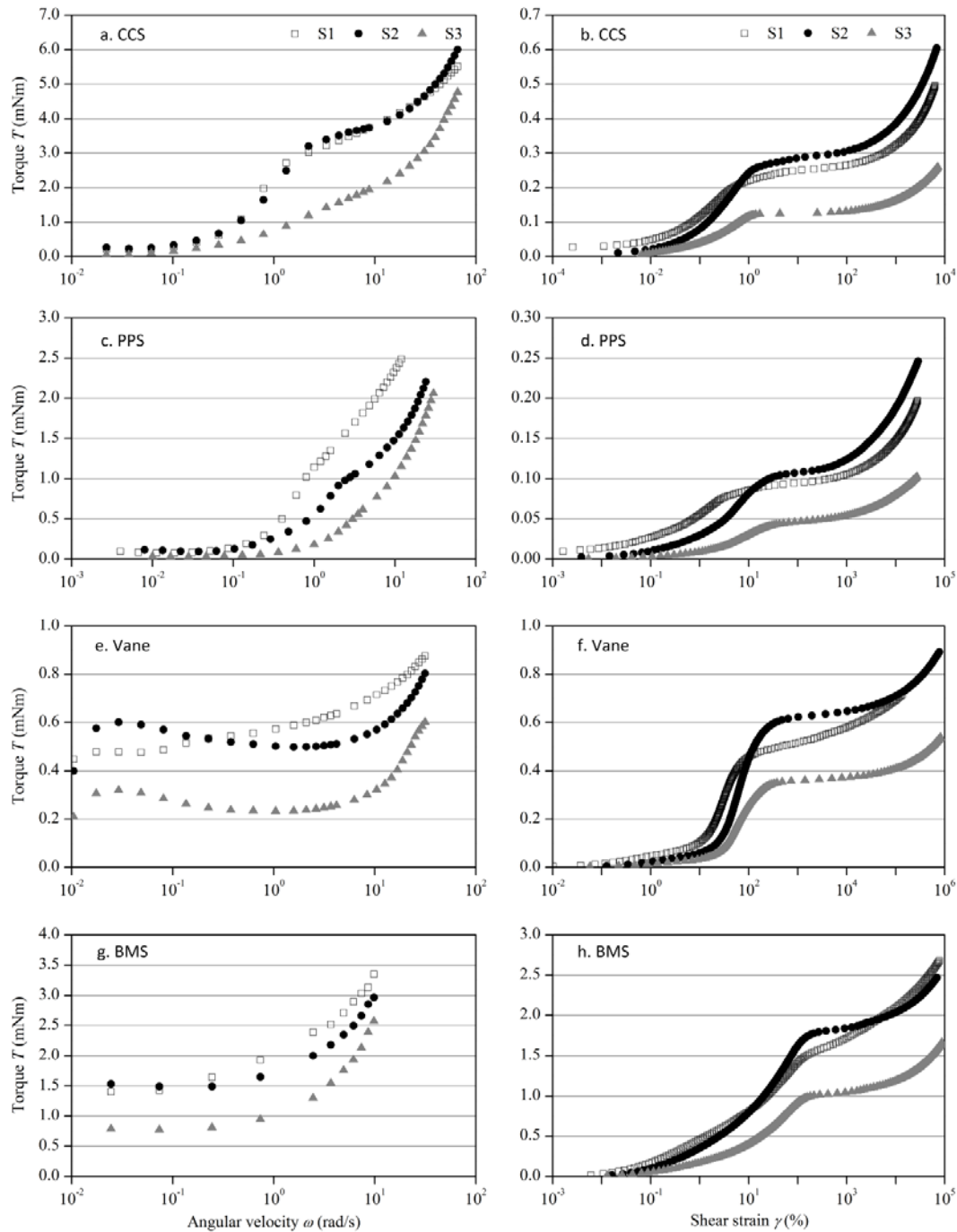
Figure 2 The torque T versus angular velocity ω (a, c, e, g) and torque T versus shear strain γ curves (b, d, f, h) from different systems.

2 mm when testing S2. Eq. 4 shows that shear rate decreases with increasing gap width. As a result, shear rate in S1 is higher than S2 at the same angular velocity for the PPS and the corresponding value of torque on S1 is larger.

As shown in Figure 2a and Figure 2c, T-ω curves from the CCS and the PPS exhibit two distinct regions: T increases rapidly with ω in the low shear region, whereas T increases slowly in the high shear region. The transition point is around ω=2 rad/s. Similar results are also found by other researchers using mud slurries and a smooth-walled CCS (Huang and Aode 2009; Jeong 2014). Jeong (2014) defined the two regions the "creep-governed" and "flow-governed" regions respectively. However, wall slip effects can also produce similar phenomenon (Barnes 1995). T-ω curves from the vane geometry and the BMS show that T generally increased with ω. Nevertheless, T-ω curves of S2 and S3 exhibit stress overshoot effect when the angular velocity is very small. This phenomenon was observed again in the special repeated test for the two samples. Therefore, it was not induced by the experimental error. The stress overshoot phenomenon was also observed by Martino (2003) in vane geometry because of formation of a consolidated zone in the bottom of the measuring cup due to settling that caused a non-uniform vertical distribution of stresses on the rotor. In the current study no appreciable particle settling was observed when cleaning the cup after each test. The overshoot effect probably indicates the decrease of the strength of the network structure of the sample (Wang et al. 2004).

Table 1 Values of yield torque (mNm) from different systems

| Sample	CCS	PPS	Vane	BMS
S1	0.252	0.094	0.511	1.583
S2	0.293	0.107	0.623	1.808
S3	0.125	0.046	0.361	1.024

Note: CCS=Concentric cylinder systems; PPS= Parallel-plate systems; BMS= ball measuring system

T-γ curves in Figure 2 show that all of the three samples behaved as yield stress fluids: γ increases slowly with T when T is small, whereas γ increases rapidly with T when T exceeds a certain value. All T-γ curves involved a relatively flat section in the semi-logarithmic graph, where log (γ) increases very fast with T, indicating that the

sample yields in this section. Therefore, the value of T corresponding to the maximum value of $\Delta\log(\gamma)/\Delta T$ is defined as yield torque T_y. Values of T_y are listed in Table 1. With any system, T_y value of S2 is the highest while T_y value of S3 is the smallest.

3.2 Shear rate and shear stress

The rheological relationship, i.e., the shear stress versus shear rate curves, can be derived from the measured data according to equations in section 2, and illustrated in Figure 3. Graphs with both linear and semi-logarithmic coordinates are given to better illustrate the flow curve in both low
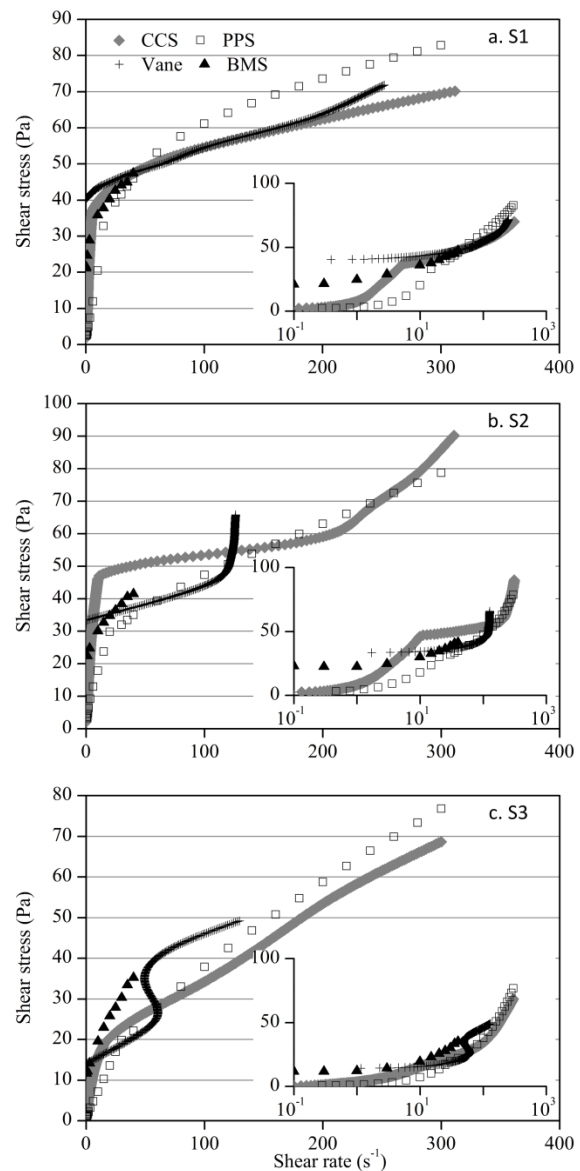
Figure 3 Flow curves from different systems.

and high shear regions. One data point in the T-ω curve corresponds to one data point in the τ-$\dot{\gamma}$ curve for the PPS and the BMS. The integral formula (Eq. 2) was converted into a discrete summation formula when converting measured data from the CCS and the vane geometry (Yeow et al. 2000), so data points in the τ-$\dot{\gamma}$ curves are much more than those in the T-ω curves. With the vane geometry, the experimental data for S2 and S3 with very small angular velocities where the T-ω curves exhibit the overshoot effect were not used in the conversion.

In general, the relative magnitude of shear stresses in different systems varies with the shear rate. In the case of low shear rate ($\dot{\gamma}$ <3 s⁻¹), shear stress levels from the vane geometry are the highest, while the CCS and the PPS give much lower shear stress levels. In the case of relatively high shear rate ($\dot{\gamma}$ >10 s⁻¹), the four systems give comparable shear stress levels.

Table 2 Values of yield stress (Pa) from different systems (Sp: Sample)

Sp	CCS	PPS	Vane	BMS	ICT
S1	3.80	2.86	41.93 (34.11)	23.75	21.2~33.4
S2	4.42	3.28	51.12 (41.59)	27.12	
S3	1.88	1.41	29.62 (24.10)	15.36	

Notes: Data in the brackets are yield stress values modified by Eq. 14

Similar to the T-ω curves shown in Figure 2c, τ-$\dot{\gamma}$ curves from the PPS involved two regions with the turning point of $\dot{\gamma}$ =15, 20, and 30 s⁻¹ for S1, S2, and S3 respectively. τ-$\dot{\gamma}$ curves from the CCS appear more complex: curves of S1 and S3 involve two sections with the turning point of $\dot{\gamma}$ =5.3 and 15 s⁻¹ separately, whereas the curve of S2 involves three sections with the turning points of $\dot{\gamma}$ =10 and 200 s⁻¹, the first point corresponding to the turning point of the T-ω curve, while occurrence of the second point requires further research. τ-$\dot{\gamma}$ curves from the vane geometry are not smooth: τ monotonically increases with $\dot{\gamma}$ for S1, however the gradient becomes greater in the region of $\dot{\gamma}$ >200 s⁻¹; for S2 the gradient increases abruptly in the region of $\dot{\gamma}$ >110 s⁻¹; the flow curve exhibits an S-shape for S3. These phenomena may be attributed to the fact that turbulent flow occurs more easily in the vane geometry than the CCS and the PPS. Flow

curves with the BMS are smooth. However, shear rate varies in a relatively small range because the linear relationship between $\dot{\gamma}$ and ω is invalid in the high shear region (Schatzmann et al. 2009).

Yield stress (Table 2) is derived from the torque data in Table 1. In order to evaluate the results, yield stress of S1 was also determined through an inclined channel test (ICT), a practical method for yield stress determination. In the test, a measured volume of slurry was poured into a tank, then the gate of the tank was opened and the slurry flowed into an inclined rectangular channel with the width of B=20 cm, and finally thickness of the deposit, h, was measured along the channel with a ruler when the flow ceased. With the deposit of uniform thickness, yield stress is computed as:

$$\tau_y = \frac{B}{B+2h}\rho g h \sin\theta \qquad (12)$$

where g is the gravitational acceleration, and θ is the inclined angle of the channel. Concerning the non-uniform thickness in our experiment, the following force balance equation was established for the fluid element with a length of Δl:

$$\rho g h B \Delta l \sin\theta + \frac{1}{2}\rho g B h_1^2 \cos\theta = \\ (B+2h)\Delta l \tau_y + \frac{1}{2}\rho g B h_2^2 \cos\theta \qquad (13)$$

where h_1 and h_2 are deposit thickness at the upstream and downstream sections of the element separately.

Yield stress from Eq. 13 varies between 21.2-33.4 Pa with an average of 27.6 Pa. Moreover, measurement error in h is about 2 mm and it produces an error of around 8% for the computed yield stress. Table 2 shows that the yield stress value from the BMS is close to the value from ICT, while the values from the CCS and the PPS are significantly smaller, indicating that slip effects existed during the measurement, which produced a pseudo yield stress region (Barnes 1995). Yield stress value from the vane geometry is clearly larger than the value from ICT. This may be induced by the end effect. When the vane geometry is used for rheological testing, two effects should be considered. The first effect is that the torque exerted on the vane is smaller than the equivalent CCS (Ovarlez et al. 2011), which means that the torque value should be enlarged if it is treated as a

CCS. The second effect is that the end of the vane also contributes to the total torque, which means that the torque value should be reduced. In the present study, a correction factor of 1.097 was obtained for torque when calibrating the vane geometry using standard silicon oil, indicating that the first effect plays more important roles than the second effect. However, the standard silicon oil is a Newtonian fluid and contribution of the end to the total torque is related with rotational speed. Distance between the lower end of the vane and the bottom wall of the measuring cup is 60 mm, which is much larger than the gap width of the shearing zone (r_o-r_i = 10 mm). Therefore, shear rate at the end of the vane is much smaller than in the gap, and contribution of the end to the total torque is relatively small for a Newtonian fluid. For a yield stress fluid, additional torque induced by the end is relatively large, which is equivalent to the PPS, and the yield stress can be computed with the following equation (Barnes and Nguyen 2001):

$$\tau_y = \frac{T_y}{2\pi r_i^3} \left(\frac{L}{r_i} + \frac{1}{3} \right)^{-1} \tag{14}$$

In our experiment, the upper end of the vane was not immersed by the sample, thus end effect only on the lower end should be considered and a ratio of 1/3 was used in Eq. 14 instead of a ratio of 2/3 as given in the original literature. Yield stress value of S1 from Eq. 14 is 34.11 Pa as given in the bracket in Table 2, which is close to the value from ICT. With S2 and S3, there were not enough samples for the inclined channel test, and the corresponding values of yield stress are absent in Table 2.

3.3 Rheological parameters

In order to further compare the rheological data from different systems, the Herschel-Bulkley model was employed to compute rheological parameters of each sample for its wide use in mud slurries (Coussot et al. 1998). According to the analysis in the previous section, rheological data from the CCS and the PPS exhibit a pseudo yield stress in the low shear region, and thus data fitting was performed only in the high shear region for these two systems. The results are listed in Table 3.

There is a clear difference between rheological parameters obtained with different systems. Since there are no standard reference values for comparison, the fitted values of yield stress were used to evaluate each system. With the vane geometry, the fitted value of τ_y is close to the corresponding value in Table 2 for S1, whereas this value is much smaller than the corresponding value in Table 2 for S2 and S3, because τ_y values determined through data fitting correspond to a dynamic state and represent residual strength of the sample structure, while values in Table 2 correspond to a static state and represent strength needed to initiate the flow. The latter is greater than the former, which agrees with the stress overshoot phenomenon as shown in Figure 2e. With the BMS, the fitted values of τ_y are 20%-30% lower than the corresponding values in Table 2. This is also probably related to decrease of the strength of the network structure of the sample. For S1, the fitted value of τ_y is 17.01 Pa. It is a little smaller than the lower limit of values from ICT (21.2 Pa). However, it still remains reasonable if measurement error is

Table 3 Rheological parameters fitted with the Herschel-Bulkley model

Sample	Measuring system	Shear rate range (s^{-1})	τ_y (Pa)	K (Pa s^n)	n	RMSE (Pa)	R^2
S1	CCS	5.3-300	29.83	3.914	0.402	0.338	0.999
	PPS	15-300	-37.38	43.043	0.179	0.341	0.999
	Vane	0-200	40.63 (33.05)	0.445	0.743	0.233	0.999
	BMS	0-40	17.01	7.900	0.362	0.435	0.998
S2	CCS	10-200	45.43	0.426	0.642	0.262	0.994
	PPS	20-300	22.90	0.715	0.762	0.380	0.999
	Vane	0-110	33.67(27.39)	0.042	1.195	0.143	0.998
	BMS	0-40	21.61	1.765	0.663	0.514	0.995
S3	CCS	15-300	16.83	0.198	0.981	0.593	0.998
	PPS	30-300	5.26	1.207	0.716	0.091	1.000
	Vane	0-50	14.16(11.52)	0.114	1.091	0.046	1.000
	BMS	0-40	11.07	1.453	0.764	0.298	0.999

Note: data in the brackets are yield stress values modified by Eq. 14.

considered. With the CCS, the fitted value of τ_y is 29.83 Pa for S1 and is close to the value from ICT (Table 2). With the PPS, the fitted value of τ_y is negative for S1, while it is close to the fitted τ_y value from the BMS for S2, whereas it is much smaller than the value from the BMS for S3. This indicates that τ_y values fitted with data alone in the high shear region may have a large error.

4   Conclusions

Soil samples with clay content ranging from 15% to 31% were taken from three debris flow gullies in Southwest China. Three debris flow slurries were prepared and tested with the concentric cylinder system, the parallel-plate system, the vane geometry, and the ball measuring system of a rheometer MCR301 respectively. The results were compared and the following conclusions are drawn: (1) wall-slip effects are prone to occur in the smooth-walled concentric cylinder and parallel-plate systems in the low shear region and can give rise to a much smaller yield stress value, whereas rheological data in the high shear region are relatively similar; (2) the vane geometry can capture the stress overshoot phenomenon, while

the yield stress value should be modified to eliminate the end effects; and (3) rheological data from the ball measuring system are reasonable, and this system is applicable for debris flow slurry measurement.

The slurries used in this study had relatively high viscosity and particle sedimentation was low during the test. For debris flows involving particles with little cohesion, particle settling should be taken into account. Further study is needed to evaluate the applicability of each rheometric device for these types of debris flow slurries.

Acknowledgements

References

Ancey C (2005) Solving the Couette inverse problem using a wavelet-vaguelette decomposition. Journal of Rheology 49: 441-460. DOI: 10.1122/1.1849181

Ancey C, Jorrot H (2001) Yield stress for particle suspensions within a clay dispersion. Journal of Rheology 45: 297-319. DOI: 10.1122/1.1343879

Barnes HA (1995) A review of the slip (wall depletion) of polymer solutions, emulsions and particle suspensions in viscometers: its cause, character, and cure. Journal of Non-Newtonian Fluid Mechanics 56: 221-251. DOI: 10.1016/0377-0257(94)01282-M

Barnes HA, Nguyen QD (2001) Rotating vane rheometry - a review. Journal of Non-Newtonian Fluid Mechanic 98: 1-14. DOI: 10.1016/S0377-0257(01)00095-7

Boyer F, Guazzelli E, Pouliquen O (2011) Unifying suspension and granular rheology. Physical Review Letters 107: 188301. DOI: 10.1103/PhysRevLett.107.188301

Chan D, Powell RL (1984) Rheology of suspensions of spherical particles in a newtonian and a non-newtonian fluid. Journal of Non-Newtonian Fluid Mechanics 15: 165-179. DOI: 10.1016/0377-0257(84)80004-X

Contreras SM, Davies TRH (2000) Coarse-grained debris flows: hysteresis and time-dependent rheology. Journal of Hydraulic Engineering 126: 938-941. DOI: 10.1061/(ASCE)0733-9429 (2000)126:12(938)

Coussot P (1995) Structural similarity and transition from Newtonian to non-Newtonian behavior for clay-water mixtures. Physical Review Letters 74: 3971-3975.

Coussot P (1997) Mudflow Rheology and Dynamics. IAHR Monograph Series.

Coussot P, Laigle D, Arattano M, et al. (1998) Direct determination of rheological characteristics of debris flow. Journal of Hydraulic Engineering 124: 865-868. DOI: 10.1061/(ASCE)0733-9429(1998)124:8(865)

Duan HJ, Sun HH (2001) New method of measuring rheologic parameters of high-density slurry. Journal of China University of Mining & Technology 30(4): 371-374. (In Chinese)

Huang N, Ovarlez G, Bertrand F, et al. (2005) Flow of wet granular materials. Physical Review Letters 94: 028301. DOI: 10.1103/PhysRevLett.94.028301

Huang Z, Aode H (2009) A laboratory study of rheological properties of mudflows in Hangzhou Bay, China. International Journal of Sediment Research 24: 410-424. DOI: 10.1016/S1001-6279(10)60014-5

Jeong SW (2014) The effect of grain size on the viscosity and yield stress of fine-grained sediments. Journal of Mountain Science 11: 31-40. DOI: 10.1007/s11629-013-2661-1

Major JJ, Pierson TC (1992) Debris flow rheology: experimental analysis of fine-grained slurries. Water Resources Research

28: 841-857. DOI: 10.1029/91WR02834

Martino R (2003) Experimental analysis on the rheological properties of a debris-flow deposit. In: Rickenmann D & Chen CL (eds.), Proceedings of the 3rd International Conference on Debris-Flow Hazards Mitigation. Davos, Switzerland. pp 363-373.

Martino R, Papa MN (2008) Variable-concentration and boundary effects on debris flow discharge predictions. Journal of Hydraulic Engineering 134: 1294-1301. DOI: 10.1061/(ASCE)0733-9429(2008)134:9(1294)

Mezger TG (2006) The Rheology Handbook: For users of rotational and oscillatory rheometers. (2nd ed). Vincentz Network, Hannover, Germany.

Müller M, Tyrach J, Brunn PO (1999) Rheological characterization of machine-applied plasters. ZKG International 52: 252-258.

Nguyen QD, Boger DV (1987) Characterization of yield stress fluids with concentric cylinder viscometers. Rheologica Acta 26: 508-515. DOI: 10.1007/BF01333734

O'Brien JS, Julien PY (1988) Laboratory analysis of mudflow properties. Journal of Hydraulic Engineering 114: 877-887. DOI: 10.1061/(ASCE)0733-9429(1988)114:8(877)

Ovarlez G, Mahaut F, Bertrand F, et al. (2011) Flows and heterogeneities with a vane tool: Magnetic resonance imaging measurements. Journal of Rheology 55: 197-223. DOI: 10.1122/1.3526349

Ren XF (1995) Calculation method of slurry rheologic parameter measured by rotary viscosimeter. Journal of Hydraulic Engineering (9): 75-81. (In Chinese)

Schatzmann M, Bezzola GR, Minor H-E, et al. (2009) Rheometry for large-particulated fluids: analysis of the ball measuring system and comparison to debris flow rheometry. Rheologica Acta 48: 715-733. DOI: 10.1007/s00397-009-0364-x

Shen SC (1998) Experiment of rheology of debris flow. Journal of Hydraulic Engineering (9): 7-13. (In Chinese)

Sosio R, Crosta GB (2009) Rheology of concentrated granular suspensions and possible implications for debris flow modeling. Water Resources Research 45: W03412. DOI: 10.1029/2008WR006920

Vanoni VA, ed. (1975) Sedimentation Engineering. ASCE, New York, USA.

Wang YY, Jan CD, Han WL, et al. (2004) Experimental research on constitutive relation of thixotropy stress of viscous debris flow. Journal of Natural Disasters 13(3): 33-38. (In Chinese)

Yeow YL, Ko WC, Tang PPP (2000) Solving the inverse problem of Couette viscometry by Tikhonov regularization. Journal of Rheology 44: 1335-1351. DOI: 10.1122/1.1308520

Yang TMT, Krieger IM (1978) Comparison of methods for calculating shear rates in coaxial viscometers. Journal of Rheology 22: 413-421. DOI: 10.1122/1.549483